

# Synthesis, Characterization, and Interconversion of the Rhenium Polyhydrides $[\text{ReH}_3(\eta^4\text{-NP}_3)]$ and $[\text{ReH}_4(\eta^4\text{-NP}_3)]^+$ $\{\text{NP}_3 = \text{tris}[2\text{-(diphenylphosphanyl)-ethylamine}]\}$

Alberto Albinati,<sup>[a]</sup> Vladimir I. Bakhmutov,<sup>\*[b]</sup> Natalia V. Belkova,<sup>[c]</sup> Claudio Bianchini,<sup>\*[d]</sup> Isaac de los Rios,<sup>[d]</sup> Lina Epstein,<sup>\*[c]</sup> Evgenii I. Gutsul,<sup>[c]</sup> Lorenza Marvelli,<sup>[e]</sup> Maurizio Peruzzini,<sup>\*[d]</sup> Roberto Rossi,<sup>\*[e]</sup> Elena Shubina,<sup>[c]</sup> Evgeni V. Vorontsov,<sup>[c]</sup> and Fabrizio Zanobini<sup>[d]</sup>

**Keywords:** Rhenium / Tripodal ligands / Phosphanes / Hydride ligands

The rhenium(III) dichloride complex  $[\text{ReCl}_2(\eta^4\text{-NP}_3)]\text{Cl}$  (**1**) was prepared from  $[\text{ReCl}_3(\text{CH}_3\text{CN})(\text{PPh}_3)_2]$  by treatment with the tripodal tetradentate ligand  $\text{N}(\text{CH}_2\text{CH}_2\text{PPh}_2)_3$  ( $\text{NP}_3$ ) in ethanol. The reaction of **1** with  $\text{LiAlH}_4$  in THF gave the rhenium(III) trihydride  $[\text{ReH}_3(\eta^4\text{-NP}_3)]$  (**2**), which was converted into the rhenium(V) tetrahydride  $[\text{ReH}_4(\eta^4\text{-NP}_3)]\text{BPh}_4$  (**3**) by protonation in  $\text{CH}_2\text{Cl}_2$  with  $\text{HBF}_4\cdot\text{OMe}_2$ , followed by a metathetical reaction with  $\text{NaBPh}_4$ . The classical polyhydride nature of **2** and **3**, as well as the overall molecular structures in solution, were determined by NMR spectroscopy,  $^1\text{H}$  NMR relaxation, and IR spectroscopy. The polyhydride complexes **2** and **3** are stereochemically nonrigid in solution, and the thermodynamic parameters associated with the fluxional processes were determined by variable-temperature NMR

studies. A single-crystal X-ray analysis of **3** has shown the complex cation  $[\text{ReH}_4(\eta^4\text{-NP}_3)]^+$  to be eight-coordinated by the four donor atoms of  $\text{NP}_3$  and by four terminal hydride ligands in a distorted dodecahedral geometry. An in situ IR study in  $\text{CH}_2\text{Cl}_2$  has shown that the protonation of **3** occurs regioselectively at the metal center with no formation of a dihydrogen complex. Kinetic hydrogen bond products of the formula  $[(\eta^4\text{-NP}_3)\text{H}_3\text{Re}\cdots\text{HOR}]$  ( $\text{ROH} = \text{C}_2\text{H}_5\text{OH}$ ,  $\text{CFH}_2\text{CH}_2\text{OH}$ ,  $\text{CF}_3\text{CH}_2\text{OH}$ ) were intercepted by IR spectroscopy at low temperature. The thermodynamic parameters associated with the formation of the hydrogen bond adducts were determined by either IR spectroscopy applying the logansen equation or van't Hoff plots of the formation constant vs. temperature.

## Introduction

In conjunction with phosphane ligands, rhenium can form stable polyhydride complexes in a variety of metal oxidation states, coordination numbers, and structures.<sup>[1]</sup> In particular, both classical ( $\text{Re}-\text{H}_x$ ) and nonclassical  $[\text{Re}-(\text{H}_2)_x]$  structures have been reported, which may contain as many as seven hydride ligands.<sup>[1]</sup> The ability to react with either dihydrogen or hydride ions from different sources makes phosphanerhenium systems effective hydro-

gen sponges. Unlike late transition metals, however, the coordinated hydrogen is not easily transferred to unsaturated substrates, which limits the application of rhenium-based catalysts in catalytic hydrogenations.<sup>[2]</sup> On the other hand, the capability to form homologous series of polyhydride complexes, often in equilibrium with each other by dihydrogen loss/uptake, confers to phosphanerhenium compounds a great potential both in hydrogen storage and transport, which will be a priority in chemistry in the next years,<sup>[3]</sup> and for model studies of hydride-containing enzymes such as nitrogenases and hydrogenases.<sup>[4]</sup> Moreover, the chemistry of rhenium is very similar to that of the germane element technetium-99, which is largely used in diagnostics and radio therapeutics.<sup>[5]</sup> Although we are not aware of any utilization of technetium-99 or rhenium-186/188 polyhydrides (polydeuterides), it cannot be excluded a priori that such compounds may have important applications in nuclear medicine.

Tripodal polyphosphane ligands are particularly amenable to forming stable polyhydride rhenium compounds due to the nucleophilicity of trivalent phosphorus as well as the ability to generate sterically congested pockets into which the metal atom is almost buried. These ligands may therefore react only with small molecules or ions.<sup>[6]</sup>

<sup>[a]</sup> Istituto Chimico, Farmaceutico e Tossicologico, Università di Milano, Milano, Italy

<sup>[b]</sup> Centro de Investigación y de Estudios Avanzados del I. P. N., Apdo postal 14-740, 07000 México D.F., México  
E-mail: vladimir@mail.cinvestav.mx

<sup>[c]</sup> A. N. Nesmeyanov Institute of Organoelement Compounds, Vavilov str. 28, V-334, Moscow, Russia, 117813  
E-mail: epst@ineos.ac.ru

<sup>[d]</sup> Istituto di Chimica dei Composti Organo Metallici, ICCOM-CNR, Via J. Nardi 39, 60132 Firenze, Italy  
E-mail: bianchini@fi.cnr.it, peruz@fi.cnr.it

<sup>[e]</sup> Dipartimento di Chimica, Università di Ferrara, Via Borsari 46, 44100 Ferrara, Italy  
E-mail: mg1@dns.unife.it

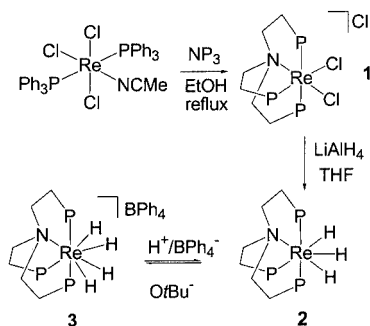
The “hydride” chemistry of rhenium with the tripodal tridentate ligand  $\text{MeC}(\text{CH}_2\text{PPh}_2)_3$  (triphos) has been intensely investigated in the last few years, leading to interesting results with regard to the formation of classical and nonclassical polyhydrides with the metal center in the oxidation states from +1 to +7.<sup>[7–9]</sup> In contrast, no rhenium complex with the potentially tetradentate aminophosphane  $\text{N}(\text{CH}_2\text{CH}_2\text{PPh}_2)_3$  ( $\text{NP}_3$ ) has been described in the literature, which is surprising as ( $\text{NP}_3$ )metal complexes are known for almost all middle and late-transition metals<sup>[6,10]</sup> including technetium.<sup>[11]</sup> A rhenium(III) tetrahydride with the tripodal phosphane ligand  $\text{P}(\text{CH}_2\text{CH}_2\text{PPh}_2)_3$  has been described, but no X-ray structure was reported.<sup>[12]</sup>

The presence of the amine nitrogen donor and of two  $\text{CH}_2$  spacers separating the phosphorus donors from the bridgehead atom makes  $\text{NP}_3$  more flexible than triphos and also increases the overall basicity at the coordinated metal center.<sup>[13,14]</sup> Ultimately, this may result in increased stability of  $\text{Re}-\text{H}_x$  moieties as well as a richer diversity of coordination geometries since  $\text{NP}_3$  may act as an  $\eta^4$ ,  $\eta^3$ - $\text{P}_3$ ,  $\eta^3$ - $\text{N}, \text{P}, \text{P}$ , and  $\eta^2$ - $\text{P}, \text{P}$  ligand.<sup>[14]</sup>

In this article we describe the synthesis, structure, and spectroscopic characterization of the first rhenium(III) and rhenium(V) polyhydride complexes stabilized by  $\text{NP}_3$ , using  $[\text{ReCl}_2(\eta^4\text{-NP}_3)]\text{Cl}$  (**1**) as a precursor. Particular attention was paid to the study of the solution structure of the complexes  $[\text{ReH}_3(\eta^4\text{-NP}_3)]$  (**2**) and  $[\text{ReH}_4(\eta^4\text{-NP}_3)]\text{BPh}_4$  (**3**), as well as the proton transfer that converts **2** into **3** via hydrogen bond adducts  $[(\eta^4\text{-NP}_3)\text{H}_3\text{Re}\cdots\text{HOR}]$ .

## Results and Discussion

The preparations and the principal reactions described in this paper are reported in Scheme 1. Selected IR spectroscopic data for the new complexes are given in the Exp. Sect. together with analytical and physicochemical properties.



Scheme 1

### Synthesis and Characterization of $[\text{ReCl}_2(\eta^4\text{-NP}_3)]\text{Cl}$ (**1**)

By reaction of  $\text{NP}_3$  with the rhenium(III) complex  $[\text{ReCl}_3(\text{CH}_3\text{CN})(\text{PPh}_3)_2]$  in refluxing ethanol, the complex  $[\text{ReCl}_2(\eta^4\text{-NP}_3)]\text{Cl}$  (**1**) was obtained in good yield as air-stable lemon-yellow microcrystals. The combined analytical, conductivity and spectroscopic characterization of **1** is

unequivocally consistent with an octahedral geometry of the complex cation  $[\text{ReCl}_2(\eta^4\text{-NP}_3)]^+$  with all the four donor atoms of  $\text{NP}_3$  coordinated to the metal center. Complex **1** is paramagnetic ( $\mu_{\text{eff}} = 2.0 \mu_{\text{B}}$ ) and thus the  $^{31}\text{P}\{^1\text{H}\}$  NMR spectrum did not provide any useful information due to the rapid relaxation of the coordinated phosphorus nuclei. The  $^1\text{H}$  NMR spectrum exhibit the typical Knight-shifted appearance<sup>[7]</sup> with relatively sharp resonances, some of which feature unusually large shifts (up to  $\delta = -40.83$ ).

### Synthesis and Characterization of the Classical Rhenium(III) and Rhenium(V) Polyhydrides $[\text{ReH}_3(\eta^4\text{-NP}_3)]$ (**2**) and $[\text{ReH}_4(\eta^4\text{-NP}_3)]\text{BPh}_4$ (**3**)

The dichloride **1** was quantitatively converted into the ivory-colored trihydride complex  $[\text{ReH}_3(\eta^4\text{-NP}_3)]$  (**2**) by treatment with a large excess (ca. 20 equiv.) of  $\text{LiAlH}_4$  in refluxing THF for 6 h. The reaction was conveniently monitored by  $^{31}\text{P}\{^1\text{H}\}$  NMR spectroscopy, which showed no intermediate species along the conversion of **1** to **2**.

Complex **2** is air-stable in both the solid state and solutions of both  $\text{CH}_2\text{Cl}_2$  and  $\text{CHCl}_3$ , in which no H/Cl exchange was observed within 24 h at room temperature. The IR spectrum contains two strong  $\nu(\text{Re}-\text{H})$  absorptions at 1949 and  $1905 \text{ cm}^{-1}$  that shifted to lower frequencies in the spectrum of the perdeuterated derivative  $[\text{ReD}_3(\eta^4\text{-NP}_3)]$  (**2-D3**) [ $\nu(\text{Re}-\text{D}) = 1399$  and  $1371 \text{ cm}^{-1}$ ,  $k_{\text{H/D}} = 1.39$ ]. The perdeuterated derivative was prepared by treating **1** with  $\text{LiAlD}_4$  in refluxing THF.

The trihydride **2** is fluxional on the NMR time scale. In  $\text{CD}_2\text{Cl}_2$ , the slow-exchange  $^{31}\text{P}\{^1\text{H}\}$  NMR spectrum was attained at  $-63^\circ\text{C}$  in the form of two broad lines at  $\delta = 52.9$  (1 P) and  $36.6$  (2 P). On increasing the temperature, the two NMR signals coalesced between  $-30$  and  $-35^\circ\text{C}$  and then transformed into a single resonance at  $\delta = 41.9$  at room temperature. The exchange process of the three phosphorus atoms matches the fluxionality of the hydride resonances. Indeed, the  $^1\text{H}$  NMR spectrum of **2** at  $-63^\circ\text{C}$  showed two hydride signals at  $\delta = -4.05$  (1 H) and  $-9.50$  (2 H) that transformed into a quadruplet at  $\delta = -7.6$  with  $J(\text{HP}) = 13.4 \text{ Hz}$  on increasing the temperature to  $22^\circ\text{C}$ . The coalescence of the hydride resonances was observed at  $-23^\circ\text{C}$  from which a free activation energy ( $\Delta G_{250\text{K}}^\ddagger$ ) of  $44.8 \text{ kJ mol}^{-1}$  could be calculated by using the Shanani Atidi-Bar–Eli approach that takes into account the different populations of the exchanging sites.<sup>[15]</sup> The low-temperature limiting spectrum of **2** points to a pentagonal-bipyramidal structure in solution (seven-coordination geometry) that has been already observed for rhenium polyhydrides.<sup>[1e,7,12]</sup>

Treatment of the trihydride **2** in THF or dichloromethane with protic acids such as  $\text{HOSO}_2\text{CF}_3$ ,  $\text{HBF}_4 \cdot \text{OMe}_2$ , or  $\text{CF}_3\text{COOH}$ , followed by a metathetical reaction with  $\text{NaBPh}_4$  in EtOH, gave off-white crystals of the classical tetrahydride complex  $[\text{ReH}_4(\eta^4\text{-NP}_3)]\text{BPh}_4$  (**3**). The protonation is reversible: the reaction with strong bases, such as  $\text{KOtBu}$ , in THF regenerated the neutral trihydride **2** quantitatively.

Compound **3** was air-stable in both the solid state and solution and behaved as a typical 1:1 electrolyte in dichloro-

methane. The solid-state IR spectrum shows a strong and sharp absorption at  $1996\text{ cm}^{-1}$  due to the  $\nu(\text{Re}-\text{H})$  vibration that shifted to  $1435\text{ cm}^{-1}$  ( $k_{\text{H/D}} = 1.39$ ) in the perdeuterated derivative  $[\text{ReD}_4(\eta^4\text{-NP}_3)]\text{BPh}_4$  (**3-D<sub>4</sub>**). It is worth noting that no H/D exchange was observed when a solution of **3** in THF or  $\text{CH}_2\text{Cl}_2$  was treated with either MeOD or  $\text{D}_2\text{O}$  even after prolonged heating to temperatures close to the boiling point (in situ NMR experiment). This behavior, which is not common for metal polyhydride complexes, is identical to that of the iron trihydride  $[\text{Fe}(\text{H})(\eta^2\text{-H}_2)(\eta^4\text{-PP}_3)]\text{BPh}_4$  containing the tripodal tetradentate ligand  $\text{P}(\text{CH}_2\text{CH}_2\text{PPh}_2)_3$ .<sup>[16]</sup> The addition of 1 equiv. of  $\text{CF}_3\text{SO}_3\text{D}$  to a  $\text{CD}_2\text{Cl}_2$  solution of **3** at ambient temperature did not result in the incorporation of deuterium. At high temperature, extensive decomposition took place to give paramagnetic material, which was not characterized further.

In keeping with the behavior of the large majority of transition metal polyhydrides,<sup>[1e]</sup> the complex cation  $[\text{ReH}_4(\eta^4\text{-NP}_3)]^+$  was stereochemically nonrigid in solution on the NMR time scale. At room temperature, the  $^{31}\text{P}\{^1\text{H}\}$  NMR spectrum in  $\text{CD}_2\text{Cl}_2$  showed a sharp ( $\omega_{1/2} \approx 4\text{ Hz}$ ) singlet resonance at  $\delta = 38.73$  associated with a fast-exchange motion of the three phosphorus atoms of  $\text{NP}_3$  ( $A_3$  spin system). An off-resonance experiment, conserving a residual coupling between the hydride ions and the phosphorus atoms, transformed the singlet into a quintuplet [ $J(\text{PH})_{\text{residual}} \approx 7\text{ Hz}$ ], and confirmed the presence of four hydride ions coordinated to the rhenium atom. On decreasing the temperature, the  $^{31}\text{P}$  NMR resonance broadened and then coalesced at ca.  $-70^\circ\text{C}$  to give a broad hump with  $\omega_{1/2} \approx 185\text{ Hz}$ . Decoalescence of the resonance occurred at a lower temperature, with formation of two distinct signals integrating 2:1. However, the decoalescence process was not complete as the resolution of the expected  $\text{AM}_2$  splitting pattern was not observed even at  $-90^\circ\text{C}$  ( $\delta = 41.85$ ,  $\omega_{1/2} = 90\text{ Hz}$ ;  $\delta = 33.69$ ,  $\omega_{1/2} = 89\text{ Hz}$ ). Assuming the occurrence of an  $A_3 \rightleftharpoons A_2M$  exchange and applying the Gutowski–Holm equation corrected for the different population of the exchanging sites, a  $\Delta G_{203\text{K}}^\ddagger$  value of  $36.8\text{ kJ mol}^{-1}$  was estimated at the coalescence temperature.<sup>[15,17]</sup>

For a further decrease in the temperature down to  $-115^\circ\text{C}$  using a 1:1 (v/v) mixture of  $\text{CD}_2\text{Cl}_2$  and  $\text{CFCl}_3$  as solvent, the lower field resonance (2 P) significantly broadened and then transformed into a broad hump that was almost merged with the baseline ( $\omega_{1/2} = 432\text{ Hz}$ ). In contrast, the signal at higher field (1 P) became sharper ( $\delta = 33.46$ ,  $\omega_{1/2} = 24\text{ Hz}$ ) without showing any fine structure, however. This NMR behavior suggests the existence of a second dynamic process responsible for the magnetically nonequivalence of the three phosphorus nuclei of  $\text{NP}_3$  and also points to an  $\text{AMX}$  splitting pattern in the slow motion regime.

Figure 1 shows the variable-temperature  $^1\text{H}$  NMR spectra in the hydride region of **3**, dissolved in a 1:1 (v/v) mixture of  $\text{CD}_2\text{Cl}_2$  and  $\text{CFCl}_3$ . At  $20^\circ\text{C}$ , the spectrum showed a narrow quadruplet [ $J(\text{HP}) = 13.1\text{ Hz}$ ] centered at  $\delta = -6.62$ , which is consistent with a complete and fast scrambling of the four hydride ions. A careful NMR integration of this signal, with respect to the aliphatic triphos reson-

ances, confirmed the presence of four hydride ligands. As the temperature was lowered, the hydride resonance lost its multiplicity ( $-20^\circ\text{C}$ ), transformed into a broad hump ( $-40^\circ\text{C}$ ,  $\omega_{1/2} = 64\text{ Hz}$ ) before finally coalescing into the baseline (ca.  $-60^\circ\text{C}$ ). Complete decoalescence of the signal occurred slightly below  $-90^\circ\text{C}$  to give two well-separated signals (integrating 1:3), which at  $-100^\circ\text{C}$  fell at  $\delta = -3.00$  ( $\omega_{1/2} = 115\text{ Hz}$ ) and  $\delta = -7.74$  ( $\omega_{1/2} = 85\text{ Hz}$ ), respectively. Below this temperature, broadening of both resonances occurred, but freezing out of the solvent did not allow us to obtain any information on the limiting spectrum.

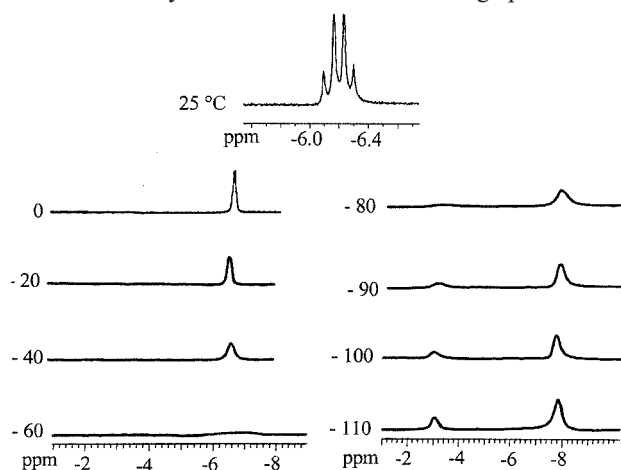
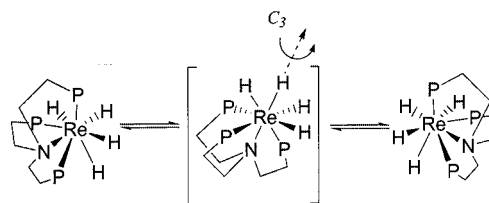


Figure 1. Variable-temperature  $^1\text{H}$  NMR spectra in the hydride region of  $[\text{ReH}_4(\eta^4\text{-NP}_3)]\text{BPh}_4$  (**3**) dissolved in a 1:1 (v/v) mixture of  $\text{CD}_2\text{Cl}_2/\text{CFCl}_3$  (300 MHz, TMS reference)

The proton NMR spectroscopic data allowed us to calculate the free energy of activation for the process of exchanging the hydride ligands in **3**. A possible mechanism for this exchanged is proposed in Scheme 2.<sup>[1e]</sup> Introducing a  $\Delta\nu$  value of  $1420\text{ Hz}$ , a  $\Delta G_{213\text{K}}^\ddagger$  value of  $38.1\text{ kJ mol}^{-1}$  was calculated at the coalescence temperature. Remarkably, this value is in good agreement with the free activation energy obtained from the NMR coalescence analysis of the  $^{31}\text{P}$  NMR spectra (vide supra). A line-shape analysis of the  $^1\text{H}$  NMR spectra (Figure 1) with the DNMR-5 program in the temperature range from 253 to 183 K gave the following  $\tau$  values for the less populated low-field signal:  $0.0000067\text{ s}$  at 253 K,  $0.000013\text{ s}$  at 233 K,  $0.00027\text{ s}$  at 213 K,  $0.0011\text{ s}$  at 193 K, and  $0.0027\text{ s}$  at 183 K. From these values we calculated  $\Delta H^\ddagger = 33.5\text{ kJ mol}^{-1}$  and  $\Delta S^\ddagger = -12.1\text{ kJ mol}^{-1}\text{ K}^{-1}$  (note that the slightly negative entropy is consistent with an intramolecular exchange) and hence  $\Delta G_{203\text{K}}^\ddagger = 36.0\text{ kJ mol}^{-1}$ , which is similar to the value obtained from the coalescence temperature.



Scheme 2

Relaxation Study of the Rhenium Polyhydrides **2** and **3**

The variable-temperature relaxation times  $T_1$  for the hydride ligands in **2** and **3** were measured at different magnetic fields by using the standard inversion-recovery sequence (Table 1).

Table 1. Variable-temperature ( $T_1$ ) NMR spectroscopic data for  $[\text{ReH}_3(\eta^4\text{-NP}_3)]$  (**2**) and  $[\text{ReH}_4(\eta^4\text{-NP}_3)]^+$  (**3**)

Temp. [K]	$T_1$ [ms]		
	A $[\text{ReH}_3(\eta^4\text{-NP}_3)]$ (400 MHz) <sup>[a][b]</sup>	B	C
203		198	182
213		142	142
223		131	133
233		130	127
243		129	148
253	140–150		
$[\text{ReH}_4(\eta^4\text{-NP}_3)]^+$ (400 MHz) <sup>[c] [b]</sup>			
203		125	133
213	96–98		
223	97		
233	98		
243	100		
253	109		
263	109		
$[\text{ReH}_4(\eta^4\text{-NP}_3)]^+$ (300 MHz) <sup>[d] [b]</sup>			
173		111	106
183		97	94
193		81	86
213	<sup>[e]</sup>		
233	77		
253	83		
273	96		
293	106		

<sup>[a]</sup> The  $T_1$  measurements on **2** were carried out at 400 MHz in  $\text{CD}_2\text{Cl}_2$ . <sup>[b]</sup> The letter A denotes the  $T_1$  values of the hydride ligands in the fast motion regime. The letters B and C indicate the relaxation times of the two kinds of hydride resonances appearing below the coalescence temperature; B, low-field resonance; C, high-field resonance. <sup>[c]</sup> The  $T_1$  measurements on **3**, prepared in situ from **2** by adding 4 equiv. of  $\text{CF}_3\text{COOH}$ , were carried out at 400 MHz in  $\text{CD}_2\text{Cl}_2$ . <sup>[d]</sup> The  $T_1$  measurements on an isolated sample of **3** were carried out at 300 MHz in a 1:1  $\text{CD}_2\text{Cl}_2/\text{CFCl}_3$  mixture. <sup>[e]</sup> Due to broadness of the signal close to the coalescence temperature, no  $T_1$  value is given.

At low temperature, when the hydride–hydride exchange is slow on the NMR time scale, the relaxation times of the two types of hydride ligands in **2** were found to be practically identical. A relatively long  $T_{1\text{min}}$  value was observed between  $-50$  and  $-40$  °C (129–127 ms) for both hydride resonances supporting the classical nature of the trihydride **2**.

The tetrahydride **3** was prepared in situ as trifluoroacetate salt by adding a fourfold excess of  $\text{CF}_3\text{COOH}$  to a  $\text{CD}_2\text{Cl}_2$  solution of **2**, and the relaxation times  $T_1$  were initially measured at 400 MHz. A rather small  $T_{1\text{min}}$  value of 97 ms was determined for the four exchanging hydride ions

at ca.  $-50$  °C. Spin-saturation transfer experiments showed the absence of any exchange between the hydride ligands of **3** and protons of the acid, even at  $-23$  °C, which strongly supports the hypothesis that the observed  $T_{1\text{min}}$  value is undistorted. A comparison of  $1/T_{1\text{min}}$  measured for both **2** and **3** allowed us to estimate the relaxation contribution to the overall relaxation rate provided by the additional hydride ligand in **3**. Using a contribution of  $2.5\text{ s}^{-1}$ , a minimum hydride–hydride distance of  $1.84\text{ \AA}$  was obtained from Equation (1), in which  $\nu$  is the spectrometer frequency.<sup>[18]</sup> The H–H separation estimated in this way nicely supports the classical tetrahydride formulation of **3** and is also consistent with the results of an X-ray structural analysis (see below).

$$r(\text{H}-\text{H}) = 5.815 (T_{1\text{min}}/\nu)^{1/6} \quad (1)$$

The interpretation of  $T_{1\text{min}}$  data in terms of bond lengths in metal polyhydride complexes is affected by a rather high degree of ambiguity, particularly when the different hydride sites cannot be completely frozen out.<sup>[19]</sup> Additional uncertainty may come also from the contribution of dipolar interactions with the neighboring nuclei in the ancillary ligands that cannot be neglected, and from the presence of a quadrupolar nucleus (i.e. rhenium) which may affect remarkably the observed relaxation rate by a significant metal hydride dipole–dipole interaction.<sup>[20,21]</sup> In the case at hand, according to the protocol of Halpern and co-workers, a  $T_{1\text{min}}$  value of ca. 97 ms can be calculated by subtracting the contributions of the rhenium atom and of as many as 12 *ortho* protons of the tripodal ligands to the relaxation rate of **3**, scaled up to 500 MHz.<sup>[20]</sup> The calculated value is in line with that reported by Crabtree and co-workers for the classical polyhydride  $[\text{ReH}_6\{\text{PhN}(\text{CH}_2\text{CH}_2\text{PPh}_2)_2\}]\text{BF}_4$  ( $T_{1\text{min}} = 93\text{ ms}$ ),<sup>[22]</sup> and also matches well the  $T_{1\text{min}}$  value of 94 ms determined by Morris and co-workers for the cognate complex  $[\text{ReH}_4(\eta^4\text{-PP}_3)]\text{BF}_4$ , for which the absence of an intact dihydrogen ligand was suggested on the basis of similar  $T_1$  arguments.<sup>[12]</sup>

In a second series of NMR experiments, the spin-lattice relaxation times for the hydride ligands in **3** were determined at 300 MHz in the temperature range from  $+20$  to  $-110$  °C in  $\text{CD}_2\text{Cl}_2/\text{CFCl}_3$ . The results were in line with those obtained using a higher magnetic field. A plot of  $T_1$  [ms] vs. temperature ( $1000/T$  [ $\text{K}^{-1}$ ]) is presented in Figure 2, while  $T_1$  data are collected in Table 1. At room temperature, when the four hydride ligands are rapidly exchanging, a relatively short  $T_1$  of 106 ms was measured. As the temperature was lowered to the coalescence point,  $T_1$  also decreased steadily, and at  $-40$  °C, just above the coalescence point, a value of 77 ms was observed. Below the coalescence temperature, the two hydride sites showed longer and comparable relaxation times that increased with decreasing temperature. At  $-100$  °C, when the dynamic process was still far from being completely frozen out,  $T_1$  values as long as 111 and 106 ms were determined for the two distinct hydride resonances. Interpolation of the whole set of data al-



lowed us to find an average  $T_{\text{min}}$  value of ca. 71 ms at  $-50^\circ\text{C}$  that agrees well, after scaling up to 400 MHz (94 ms), with the relaxation data obtained at higher magnetic field carried out in  $\text{CD}_2\text{Cl}_2$  solution (97 ms).

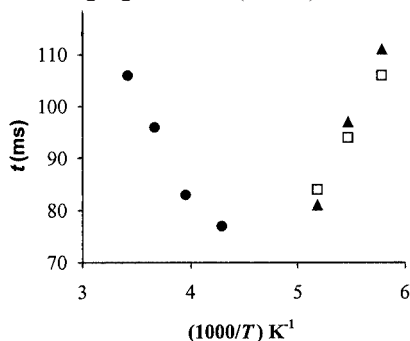


Figure 2. Plot of  $T_1$  [ms;  $\text{CD}_2\text{Cl}_2/\text{CFCl}_3$ , 1:1 (v/v), 300 MHz] vs. temperature ( $1000/T$  [ $\text{K}^{-1}$ ]) for the polyhydride  $[\text{ReH}_4(\eta^4\text{-NP}_3)]\text{BPh}_4$  (**3**); •  $T_1$  values of the four hydride atoms in the fast-exchange motion ( $\delta = -6.62$ ); □  $T_1$  values of the hydride signal ( $\delta = -3.00$ ); ▲  $T_1$  values of the hydride signal ( $\delta = -7.74$ )

Further support for the classical nature of **3** was obtained from a comparison of its variable-temperature  $T_1$  dependence with that exhibited by the authentic  $\eta^2\text{-H}_2$  complex  $[\text{Ir}(\text{H})_2(\text{H}_2)(\text{triphos})]^+$  [triphos =  $\text{CH}_3\text{C}(\text{CH}_2\text{PPh}_2)_3$ ].<sup>[23]</sup> Below the coalescence point, the  $T_1$  times for the two types of hydrides in **3** were found to lengthen considerably (Table 1), while the values for the two hydride ions in the iridium complex with triphos<sup>[23]</sup> showed a divergent behavior: the relaxation time of the classical hydrides increased, while that of the molecular hydrogen ligand continued to decrease with the temperature.

#### X-ray Crystal Structure of $[\text{ReH}_4(\eta^4\text{-NP}_3)]\text{BPh}_4$ (**3**)

An ORTEP view of the cation  $[\text{ReH}_4(\eta^4\text{-NP}_3)]^+$  is given in Figure 3, while selected bond lengths and angles are listed in Table 2. The immediate coordination sphere of the rhenium atom consists of the nitrogen and phosphorus atoms of the  $\text{NP}_3$  moiety and of four hydride ligands. As previously discussed (see Exp. Sect.), only three out of the four hydride ions (labeled as H1, H2, and H3 in Figure 3) were successfully refined. The fourth (H4) is also shown (in the position obtained from the Fourier difference map) to give a pictorial representation of the full coordination polyhedron.

As expected<sup>[24,25]</sup> for an eight-coordinated polyhydride, complex **3** adopts a distorted dodecahedral geometry in accordance with the  $^1\text{H}$  NMR spectroscopic data. The Re–H distances [av. 1.67(7) Å] fall in the expected range, and are similar to those found by low-temperature neutron diffraction in  $[\text{ReH}_5(\text{PPh}_3)_2(\text{indole})]^{[26]}$  [av. 1.683(2) Å].

The expected low precision in the location of the hydride ions by X-ray diffraction, prevents a detailed discussion of their geometries. We note, however, that the H...H separations are consistent with both the NMR spectroscopic data and the classical nature of this complex.

Two types of Re–P distances have been found in the complex cation: two shorter [av. 2.376(7) Å] and one longer

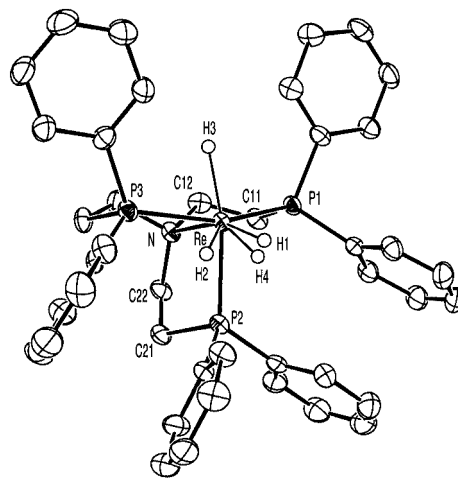


Figure 3. ORTEP view of the complex cation  $[\text{ReH}_4(\eta^4\text{-NP}_3)]\text{BPh}_4$  (**2**) showing thermal ellipsoids at 30% probability; only H1, H2, and H3 have been refined (see text)

Table 2. Selected bond lengths [Å] and angles [ $^\circ$ ] for compound **3**, with e.s.d.s values in parentheses

Re–P(1)	2.381(2)	Re–Hy1	1.60(5)
Re–P(2)	2.402(2)	Re–Hy2	1.66(5)
Re–P(3)	2.371(2)	Re–Hy3	1.79(9)
Re–N	2.309(5)		
P(1)–Re–P(2)	98.48(6)	P(1)–Re–Hy1	96(2)
P(1)–Re–P(3)	154.98(6)	P(1)–Re–Hy2	144(2)
P(1)–Re–N	81.5(1)	P(1)–Re–Hy3	85(2)
P(2)–Re–N	81.1(1)	P(2)–Re–Hy3	166(2)
P(2)–Re–P(3)	96.11(6)		
P(3)–Re–N	80.8(1)		

[2.402(2) Å] due to the influence of a pseudo-*trans*-hydride ion. All Re–P separations fall in the expected range and are comparable, for example, with those found in (triphos)-iridium complexes (2.30–2.40 Å)<sup>[27,28]</sup> All the other distances are unexceptional and do not deserve additional comment.

#### In situ IR Study of the Interaction of **2** with Different Proton Donors

It has been recently demonstrated that proton-transfer reactions such as that occurring in the transformation of **2** into **3** may take place via intermediate species containing  $\text{M} \cdots \text{H} \cdots \text{HOR}$  hydrogen bonds.<sup>[29,30]</sup> A successful strategy to show the eventual formation of hydrogen bond adducts involves an in situ IR study of the interactions between the starting metal (poly)hydride and acids of different strength. We therefore decided to monitor the reactions of **2** with  $\text{C}_2\text{H}_5\text{OH}$ ,  $\text{CFH}_2\text{CH}_2\text{OH}$  (MFE),  $\text{CF}_3\text{CH}_2\text{OH}$  (TFE),  $\text{CH}_2\text{ClCOOH}$  (MCIA), and  $\text{CF}_3\text{COOH}$  (TFA) by variable-temperature IR spectroscopy in  $\text{CH}_2\text{Cl}_2$ , taking into consideration the variation of the dielectric constant of the solvent with temperature.<sup>[30–32]</sup>

In the absence of added acid, the IR spectrum of **2** exhibits a complicated absorbance pattern in the  $\nu(\text{M} \cdots \text{H})$  region, which is a common feature to many transition metal

polyhydrides.<sup>[33,34]</sup> After removing the contribution due to the overtones of the phenyl rings using the spectra of **1** and **2-D<sub>3</sub>**, the spectrum showed the presence of three overlapped  $\nu(\text{Re-H})$  bands (1866, 1938, and 1977  $\text{cm}^{-1}$ ) whose intensities increased with decreasing temperature down to 200 K (see Figure 4a).

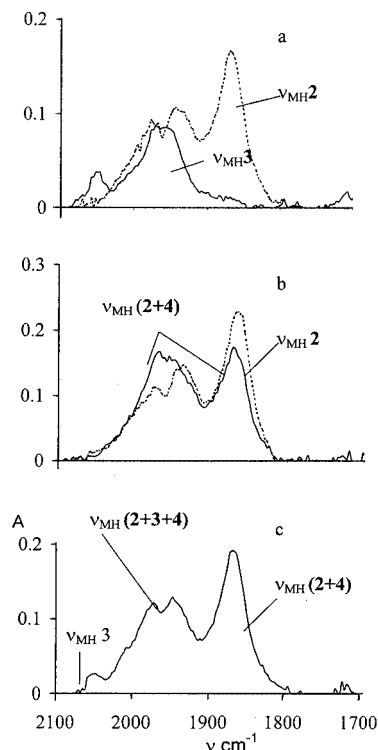


Figure 4. IR spectra in the  $\nu(\text{ReH})$  region ( $\text{CH}_2\text{Cl}_2$  solution;  $-70^\circ\text{C}$ ): a: spectra of **2** alone (0.01 M) (---) and in the presence of TFA (0.01 M) (—); b: spectra of **2** alone (0.015 M) (---) and in the presence of MFE (0.075 M) (—); c: spectrum of **2** (0.014 M) in the presence of TFE (0.014 M)

When a strong proton donor such as TFA or  $\text{MClA}$  was treated with **2** (metal hydride/acid, 1:1), a plain proton transfer occurred and the classical polyhydride **3** was generated with no detection of any intermediate species along the proton transfer process, i.e. the  $\nu(\text{ReH})$  stretching of **2** disappeared with concomitant formation of new bands due to **3** at higher energy [1960 (vs)  $\text{cm}^{-1}$  and 2050 (w)  $\text{cm}^{-1}$ ] (see Figure 4a). The latter band was masked by the phenyl overtones of the tetraphenylborate anion in the solid-state spectrum. In addition, the typical  $\nu(\text{CO})$  bands of free  $\text{MClA}$  (1730–1720  $\text{cm}^{-1}$ ) and TFA (1810–1780  $\text{cm}^{-1}$ ) were replaced by new strong  $\nu^{\text{as}}(\text{OCO})$  bands due to the carboxylate anions at 1620 and 1685  $\text{cm}^{-1}$ , respectively.

In an attempt to intercept a hydrogen bond adduct, weaker acids were used in the protonation of **2**. Indeed, irrespective of the hydrogen donor, the IR spectra in the  $\nu(\text{OH})$  region obtained at 290 K by addition of **2** (0.04 M) to  $\text{CH}_2\text{Cl}_2$  solutions containing TFE,  $\text{C}_2\text{H}_5\text{OH}$ , or MFE (Table 3)<sup>[35]</sup> showed that the intensity of the band due to the stretching vibrations of the OH group in the free acid decreased, while a new broad and intense band, assigned to a hydrogen-bonded adduct, appeared at lower frequency.

The frequency shifts [ $\Delta\nu = \nu(\text{OH})^{\text{free}} - \nu(\text{OH})^{\text{bonded}}$ ] was found to increase with the proton-donor ability of the alcohol in the order  $\text{C}_2\text{H}_5\text{OH} < \text{MFE} < \text{TFE}$ .

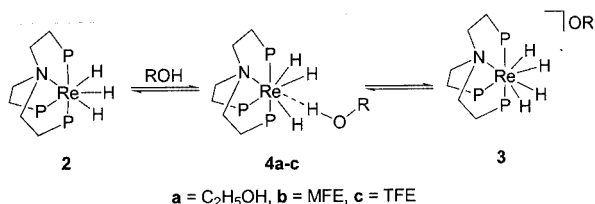
Table 3. Spectral characteristics of the hydrogen bond adducts  $[(\text{NP}_3)\text{H}_3\text{Re}\cdots\text{HOR}]$  (**4a–c**), enthalpy values ( $-\Delta H^0$ ) in  $\text{CH}_2\text{Cl}_2$  at 290 K and  $E_j$  factors

$[(\text{NP}_3)\text{H}_3\text{Re}\cdots\text{HOR}]$	$\nu(\text{OH})^{\text{bonded}}$ [ $\text{cm}^{-1}$ ]	$\Delta\nu_{\text{OH}}$ [ $\text{cm}^{-1}$ ]	$-\Delta H^0$ [ $\text{kJ mol}^{-1}$ ]	$E_j$
$\text{C}_2\text{H}_5\text{OH}$ ( <b>4a</b> )	3375	212	18.8	1.45
MFE ( <b>4b</b> )	3336	244	20.5	1.47
TFE ( <b>4c</b> )	3220	385	26.4 (24.7) <sup>[a]</sup>	1.53 (1.45)

<sup>[a]</sup> The  $-\Delta H^0$  value given in parentheses was obtained from the van't Hoff plot (Figure 5).

Once it had been established that the proton-transfer reaction involved in converting **2** to **3** was traversed by a detectable H-bonded intermediate, it only remained to discriminate between the two potential H bond acceptor sites in **2**, i.e. the hydride ligand or the metal center.<sup>[36]</sup> In reality, although the intermediacy of hydrogen bond adducts of the type  $\text{ReH}\cdots\text{HX}$ , preceding the formation of nonclassical  $\eta^2\text{-H}_2$  species, have been reported to occur in several cases,<sup>[29,30,37–40]</sup> the rhenium center in **2** possesses a lone electron pair that may be straightforwardly protonated to give the classical hydride **3**. Accordingly, we could not disregard a priori the preliminary formation of a metal-centered  $\text{Re}\cdots\text{HX}$  adduct upon interaction of **2** with the alcohol.

The occurrence of a low frequency shift of the  $\nu(\text{M-H})$  band has been unequivocally established as a general spectroscopic criterion to assess the formation of hydrogen bonding involving the hydride ligand.<sup>[29,30]</sup> In the present case, the addition of a weak proton donor such as  $\text{EtOH}$ , MFE, or TFE to a  $\text{CH}_2\text{Cl}_2$  solution of **2** did not result in the appearance of any new band or shoulder at low frequency. In contrast, either of these alcohols at  $-70^\circ\text{C}$  caused a little, but evident, high frequency shift (ca. 10  $\text{cm}^{-1}$ ) of the  $\nu(\text{Re-H})$  band at 1866  $\text{cm}^{-1}$  as well as the envelop of the two other absorptions between 1945 and 1980  $\text{cm}^{-1}$  (see Figure 4b). These spectral changes are therefore inconsistent with an interaction between a  $\text{Re-H}$  moiety and the proton donor, whereas they support the formation of hydrogen-bonded adducts of the type  $[(\text{NP}_3)\text{H}_3\text{Re}\cdots\text{HOR}]$  (**4a–c**) as shown in Scheme 3. The occurrence of a metal-centered hydrogen bonding preceding the protonation of the metal atom has been demonstrated for a few organometallic compounds.<sup>[41–44]</sup>



Scheme 3

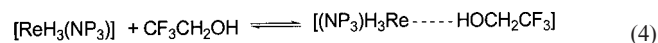
The enthalpy associated with the hydrogen bond formation in the  $\text{Re}\cdots\text{HOR}$  adducts (**4a–c**) was calculated from the experimental IR frequency shifts listed in Table 3 through the Iogansen correlation<sup>[45]</sup> reported in Equation (2).

$$-\Delta H^\circ = 18 \Delta \nu / (720 + \Delta \nu) \quad (2)$$

In the case of **4c**, it was difficult to accurately determine the position of  $\nu(\text{OH})^{\text{bond}}$ , because this band fell close to the  $\nu(\text{CH})$  bands of both **2** and the  $\text{CH}_2\text{Cl}_2$  solvent. The thermodynamic parameters for **4c** were therefore independently calculated from the temperature dependence of the formation constant ( $K_f$ ) using the van't Hoff Equation (3).

$$\ln K_f = -\Delta H^\circ / RT + \Delta S^\circ / R \quad (3)$$

The formation constant  $K_f$  for the equilibrium illustrated in Equation (4) was determined in the temperature range from +20 to –30 °C following the decrease in the optical density of the band assigned to the free OH group.



The corresponding van't Hoff plot, shown in Figure 5, allowed us to figure out both the enthalpy and entropy changes [ $-\Delta H^\circ = 24.7 \pm 1.3 \text{ kJ mol}^{-1}$ ,  $-\Delta S^\circ = 56.5 \pm 2.1 \text{ kJ mol}^{-1} \text{ K}^{-1}$ ]. Notably, the value of  $-\Delta H^\circ$  calculated from the van't Hoff plot is close to that independently obtained by using Equation (2) (Table 3).

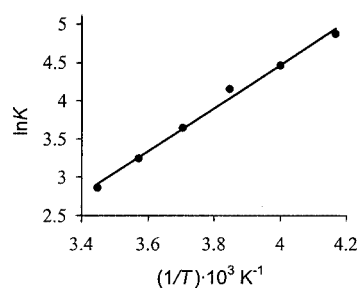


Figure 5. van't Hoff plot in the range +20 to –30 °C for the reaction of **2** with TFE

Table 3 also lists the basicity factors  $E_j$  relative to the different proton donors used in this study that were calculated by using the “rule of factors” [Equation (5)].<sup>[46]</sup>

$$E_j = \Delta H_{ij} / \Delta H_{11} P_i \quad (5)$$

The  $E_j$  values for **2** are practically constant ( $1.46 \pm 0.01$ ) for all the three proton donors listed in Table 3. Remarkably, the proton-accepting ability of the rhenium atom appeared to be higher than the  $E_j$  values previously determined for other metal-containing complexes.<sup>[29,30]</sup> Such a high  $E_j$  value for **2** might explain why the proton transfer

was observed even in the presence of relatively weak proton donors such as TFE.

The study of the interaction of **2** with TFE at different temperatures and concentrations allowed us to observe the multiple equilibrium between the initial hydride **2**, the hydrogen bond adducts **4c**, and the final product **3** (Scheme 3). This equilibrium is significantly shifted to the right at either low temperature or high TFE concentrations. The solution IR spectrum of **2** in the presence of TFE at –70 °C is very complicated (see Figure 4c): the band at  $1877 \text{ cm}^{-1}$  was assigned to the  $\nu(\text{ReH})$  stretching of both the H-bonded complex **4c** and the starting hydride **2**, the band at  $2050 \text{ cm}^{-1}$  could be assigned to the  $\nu(\text{ReH})$  of **3**, while the broad absorbance between  $1940$  and  $1970 \text{ cm}^{-1}$  was attributed to the envelope of  $\nu(\text{ReH})$  bands due to the three rhenium species in equilibrium (Scheme 3). There is little doubt, however, that the spectral changes occurring in the  $\nu(\text{MH})$  region, following the addition of TFE to a solution of **2**, unequivocally point to the rhenium atom as the site where the hydrogen bond interaction with the proton donor primarily occurs.

A recently reported ab initio study of the protonation of  $[\text{CpRe}(\text{PH}_3)(\text{NO})(\text{H})]$  and  $[\text{CpRe}(\text{CO})(\text{NO})(\text{H})]$  has shown that the substitution of CO by  $\text{PH}_3$  increases the rhenium basicity and hence shifts the regioselectivity of proton attack from the terminal hydride ion to the metal center.<sup>[47]</sup> The remarkable nucleophilic character of the  $\text{NP}_3$  ligand would analogously increase the basicity of the rhenium center in **2**, thus allowing for its regioselective protonation. As a matter of fact, the less electron-rich complex  $[\text{ReH}(\text{CO})_2(\text{triphos})]$  has been found to react with various proton donors forming selectively  $\text{ReH}\cdots\text{HOR}$  adducts.<sup>[38,39]</sup>

## Conclusions

We have described in this work the synthesis and characterization of the first rhenium polyhydride complexes stabilized by the tripodal polydentate ligand  $\text{N}(\text{CH}_2\text{CH}_2\text{PPh}_2)_3$  ( $\text{NP}_3$ ). In both  $[\text{ReH}_3(\eta^4\text{-NP}_3)]$  (**2**) and  $[\text{ReH}_4(\eta^4\text{-NP}_3)]\text{BPh}_4$  (**3**) the polydentate ligand uses all its donor atoms for coordination. The classical polyhydride structure of **2** and **3** has been unambiguously determined by a variety of spectroscopic techniques in solution as well as a single-crystal X-ray analysis of the rhenium(V) derivative. Most importantly, an in situ IR study of the protonation of **2** by weak Brønsted acids has shown that the proton selectively attacks the metal atom to give kinetic hydrogen-bonded adducts of the formula  $[(\eta^4\text{-NP}_3)\text{H}_4\text{Re}\cdots\text{HOR}]$  ( $\text{ROH} = \text{C}_2\text{H}_5\text{OH}$ ,  $\text{CFH}_2\text{CH}_2\text{OH}$ ,  $\text{CF}_3\text{CH}_2\text{OH}$ ) that ultimately convert into the thermodynamically stable classical polyhydride **3** with no formation of transient  $\eta^2\text{-H}_2$  species.

## Experimental Section

**General Procedures:** Tetrahydrofuran (THF) and diethyl ether were purified by distillation from  $\text{LiAlH}_4$  under nitrogen, dichlorome-

thane was heated under reflux overnight in the presence of  $P_2O_5$  and distilled just prior of use. All other reagents and chemicals were reagent grade and, unless otherwise stated, were used as received from commercial suppliers. All reactions and manipulations were routinely performed under dry nitrogen by using standard Schlenk-tube techniques. The solid complexes were collected on sintered-glass frits and washed as indicated before being dried in a stream of nitrogen. The ligand  $N(CH_2CH_2PPh_2)_3$  ( $NP_3$ )<sup>[48]</sup> and the complex  $[ReCl_3(CH_3CN)(PPh_3)_2]$ <sup>[49]</sup> were prepared as described in the literature. Deuterated solvents for NMR measurements (Merck and Aldrich) were dried with molecular sieves (4 Å).  $^1H$  NMR spectra were recorded with Varian VXR 300 or Bruker AC200 spectrometers operating at 299.94 or 200.13 MHz ( $^1H$ ), respectively. Peak positions are relative to tetramethylsilane and were calibrated against the residual solvent resonance.  $^{31}P\{^1H\}$  NMR spectra were recorded with either the Varian VXR 300 or Bruker AC200 instruments operating at 121.42 and 81.01 MHz, respectively. Chemical shifts were measured relative to external 86%  $H_3PO_4$  with downfield values taken as positive. The proton NMR spectra with broad-band phosphorus decoupling were recorded with the Bruker AC200 instrument equipped with a 5-mm inverse probe and a BFX-6 amplifier device using the wideband phosphorus decoupling sequence GARP. The variable-temperature spin-lattice relaxation times ( $T_1$ ) in complexes **2** and **3** were measured in dichloromethane at 300 and 400 MHz by the inversion-recovery method using the standard  $180^\circ - \tau - 90^\circ$  pulse sequence. The calculations of the relaxation times were made using the fitting routines of the Varian VXR300 and Bruker AMX-400 spectrometers. The  $90^\circ$  pulse on the hydride samples was carefully measured at each temperature before running the  $T_1$  measurements. The errors in  $T_1$  determinations were less than 10%. Infrared spectra were recorded as Nujol mulls with a Perkin–Elmer 1600 series FT-IR spectrometer between KBr plates. The molar conductivity of **1** was measured with an AMEL model 134 conductance cell connected to a model 101 conductivity meter. The conductivity data were obtained at sample concentrations of  $10^{-3}$  M in MeOH at room temperature (25 °C). Elemental analyses (C, H, N) were performed by using a Carlo Erba model 1106 elemental analyzer. IR measurements in  $CH_2Cl_2$  were carried out with a Specord M82 spectrometer in  $CaF_2$  cells. The cell width was 0.04–0.12 cm. The concentration range of the solutions for IR studies was between  $10^{-1}$  and  $10^{-3}$  M. For the low-temperature measurements a Carl Zeiss Jena cryostat was employed in the temperature range –80 to 30 °C using a stream of liquid nitrogen. The accuracy of temperature adjustment was  $\pm 0.5$  °C. The position of  $\nu(OH)$  bands corresponds to their barycenter. The formation constants at every temperature (–30 to +20 °C) were determined by the decrease of  $\nu(OH)$  optical density of the absorption band assigned to the free OH group.

**[ $ReCl_2(\eta^4-NP_3)Cl$  (**1**):** A suspension of  $[ReCl_3(CH_3CN)(PPh_3)_2]$  (0.30 g, 0.36 mmol) and  $NP_3$  (0.30 g, 0.46 mmol) in ethanol (60 mL) was heated under reflux under nitrogen for ca. 4 h, during which time the orange solid dissolved to give a clear yellow solution. The solution was then reduced in volume to ca. 20 mL before adding diethyl ether (30 mL) whilst stirring to precipitate **1** as lemon-yellow microcrystals. Yield, based on Re 0.27 g, 0.29 mmol (80%).  $C_{42}H_{42}Cl_3NP_3Re$  (875.38): calcd. C 53.3, H 4.5, N 1.5; found C 53.2, H 4.4, N 1.1.  $\Lambda_{M(methanol)} = 146 \Omega^{-1} cm^2 mol^{-1}$ .

**[ $ReH_3(\eta^4-NP_3)$  (**2**):** Solid  $LiAlH_4$  (0.64 g, 16.86 mmol) was added portionwise to a stirred suspension of **1** (0.80 g, 0.85 mmol) in 100 mL of THF. The mixture was gently heated to reflux temperature and stirred for 6 h. After cooling to 0 °C, the excess  $LiAlH_4$

was carefully hydrolyzed by addition of a mixture of THF/ $H_2O$  (30 mL, 10:1, v/v). The resulting slurry was filtered through a Hirsch funnel to remove the lithium and aluminum hydrolysis products. The volume of the filtrate was reduced to ca. 20 mL before adding 20 mL of a 1:2 (v/v) EtOH/*n*-hexane solution. Concentration of the solution under a stream of nitrogen gave ivory-colored microcrystals of **2**. Yield, 0.53 g, 0.63 mmol (74%).  $C_{42}H_{45}NP_3Re$  (842.95): calcd. C 59.8, H 5.4, N 1.7; found C 60.1, H 5.5, N 1.6. IR (Nujol mull):  $\tilde{\nu} = 1949$  ( $\nu_{ReH}$ ), 1905  $cm^{-1}$ . The perdeuterated derivative  $[ReD_3(\eta^4-NP_3)]$  (**2-D<sub>3</sub>**) was prepared with an isotopic purity higher than 90% ( $^1H$  NMR) by substituting  $LiAlD_4$ ,  $D_2O$ , and  $C_2H_5OD$  for the protonated analogues in the above procedure.

**[ $ReH_4(\eta^4-NP_3)BPh_4$  (**3**):** A Schlenk tube was charged with 0.50 g of **2** (0.59 mmol) and 10 mL of degassed dichloromethane. To this solution, cooled to 195 K with a dry ice/acetone bath, was added via syringe an excess of  $HBPh_4 \cdot OMe_2$  (0.2 mL, 1.6 mmol), and the temperature was raised to ca. 20 °C before adding a solution of  $NaBPh_4$  (0.50 g, 1.46 mmol) in EtOH (5 mL) whilst stirring. Concentration under nitrogen gave off-white crystals of **3**. Colorless plates of **3** were obtained by slow crystallization from a diluted  $CH_2Cl_2$ /EtOH (2:1, v/v) solution. Yield 0.63 g, 0.54 mmol (92%).  $C_{66}H_{66}BNP_3Re$  (1163.20): calcd. C 68.2, H 5.7, N 1.2; found C 68.6, H 5.9; N 1.2. IR (KBr):  $\tilde{\nu} = 2030$  w, br. ( $\nu_{ReH}$ ), 1996 m br.;  $\nu_{BPh_4}$  1680, 610  $cm^{-1}$ . The perdeuterated derivative  $[ReD_4(\eta^4-NP_3)BPh_4]$  (**3-D<sub>4</sub>**) was prepared with an isotopic purity higher than 95% ( $^1H$  NMR) from **2-D<sub>3</sub>** by using  $CF_3OSO_2D$  and  $C_2H_5OD$  in place of  $HBPh_4$  and ethanol.

**Reaction of **3** with  $KORu$ :** Addition of solid  $KORu$  (0.20 g, 1.78 mmol) to a THF solution of **3** (0.20 g, 0.17 mmol) regenerated the neutral trihydride **2**. Yield 89%.

**X-ray Crystallography:** Single crystals of **3** suitable for an X-ray diffraction analysis were obtained as described above. A crystal was mounted on a glass fiber, on a CAD4 diffractometer, which was used for the space group determination and for the data collection, which was carried out at –80(2) °C. Unit cell dimensions were obtained by least-squares fit of the 2 $\theta$  values of 25 high-order reflections. Crystallographic and other relevant data are listed in Table 4. Data were measured with variable scan speed to ensure constant statistical precision on the collected intensities. Three standard reflections were used to check the stability of the crystals and of the experimental conditions and measured every hour. The collected intensities were corrected for Lorentz and polarization factors and empirically ( $\Psi$  scans) for absorption.<sup>[50]</sup> The standard deviations on intensities were calculated in terms of statistics alone. The structure was solved by a combination of Patterson and Fourier methods and refined by full-matrix least squares<sup>[51]</sup> {the function minimized being  $\Sigma[w(F_o - 1/kF_c)^2]$ }. All non-hydrogen atoms were treated anisotropically. Towards the end of the refinement, four strong peaks were found, in a Fourier difference maps, at distances consistent with those expected for the hydrido ligands. Therefore these peaks were included in the refinement and treated isotropically. However, while three hydrogen atoms converged to give a reasonable geometry, maintaining also positive values for the displacement parameters, the fourth gave an Re–H separation that was considered too short, as well as a negative thermal factor, and thus was discarded. No other acceptable peak for the missing hydride ion was found in the Fourier difference maps. No extinction correction was deemed necessary. The scattering factors used, corrected for the real and imaginary parts of the anomalous dispersion, were taken from the literature.<sup>[52]</sup> The contribution of the hydrogen atoms in calculated positions [ $C-H = 0.95$  Å,  $B(H) = 1.3$



$\times B(C_{\text{bonded}}) \text{ \AA}^2]$  was taken into account but not refined. Upon convergence no significant features were found in the Fourier difference maps of both compounds. A selection of bond lengths and angles is given in Table 2 (vide infra). All calculations were performed using the MOLEN crystallographic package,<sup>[51]</sup> and the structures drawn using the program ORTEP.<sup>[53]</sup> The supplementary crystallographic data for this paper are contained in publication CCDC-179058. These data can be obtained free of charge at [www.ccdc.cam.ac.uk/contents/retrieving.html](http://www.ccdc.cam.ac.uk/contents/retrieving.html) or from the Cambridge Crystallographic Data Centre, 12, Union Road, Cambridge CB2 1EZ, UK [Fax: (internat.) + 44-1223/336-033; E-mail: [deposit@ccdc.cam.ac.uk](mailto:deposit@ccdc.cam.ac.uk)].

Table 4. Experimental data for the X-ray diffraction study of compound **3**

Empirical formula	C <sub>67</sub> H <sub>64</sub> BCl <sub>2</sub> NP <sub>3</sub> Re
Formula mass	1244.10
<i>T</i> [°C]	−80(2)
Crystal system	triclinic
Space group	<i>P</i> $\bar{1}$
<i>a</i> [Å]	12.358(2)
<i>b</i> [Å]	14.871(2)
<i>c</i> [Å]	16.545(6)
$\alpha$ [°]	107.04(3)
$\beta$ [°]	91.98(3)
$\gamma$ [°]	91.44(2)
<i>V</i> [Å <sup>3</sup> ]	2903(1)
<i>Z</i>	2
$\rho_{\text{calcd.}}$ [g cm <sup>−3</sup> ]	1.42
$\mu$ [cm <sup>−1</sup> ]	23.35
Radiation	Mo- <i>K</i> $\alpha$ (graphite-monochromated, $\lambda = 0.71069 \text{ \AA}$ )
No. independent data collected	8793
No. observed reflections	7762
	$[ I_o  > 3.5\sigma(I)]$
Transmission coeff.	1.00–0.94
<i>R</i> <sup>[a]</sup>	0.033
<i>R</i> <sub>w</sub>	0.066
GOF	1.55

<sup>[a]</sup>  $R = \Sigma(|F_o| - (1/k)F_c)/\Sigma|F_o|$ ;  $R_w = [\Sigma_w(F_o - (1/k)F_c)^2/\Sigma_w|F_o|^2]^{1/2}$ , where  $w = [\sigma^2(F_o)]^{-1}$ ;  $\sigma(F_o) = [\sigma^2(F_o^2) + f^4(F_o^2)]^{1/2}/2F_o$ .

## Acknowledgments

Thanks are due to INTAS (contract 00-00179), NATO (contract HTECH-CRG 972135), CNR/RAS bilateral agreement and RFBR (project No 99-03-33270) for financial support. Support from the EC (RTN network HYDROCHEM) is also gratefully acknowledged. I. d. I. R. thanks the Ministerio de Ciencia y Tecnología (Spain) for a post-doctoral grant.

<sup>[1]</sup> See for example: <sup>[1a]</sup> D. Gusev, A. Llamazares, G. Artus, H. Jacobsen, H. Berke, *Organometallics* **1999**, *18*, 75. <sup>[1b]</sup> G. Albertin, S. Antoniutti, S. Garcia-Fontán, R. Carballo, F. Padoan, *J. Chem. Soc., Dalton Trans.* **1998**, 2071. <sup>[1c]</sup> D. M. Heinekey, M. H. Voges, D. M. Barnhart, *J. Am. Chem. Soc.* **1996**, *118*, 10792. <sup>[1d]</sup> Y. Kim, H. Deng, J. C. Gallucci, A. Wojcicki, *Inorg. Chem.* **1996**, *35*, 7166. <sup>[1e]</sup> D. G. Gusev, H. Berke, *Chem. Ber.* **1996**, *129*, 1143 and references therein. <sup>[1f]</sup> X. L. R. Fontaine, T. P. Layzell, B. L. Shaw, *J. Chem. Soc., Dalton Trans.* **1994**, 917. <sup>[1g]</sup> X.-L. Luo, R. H. Crabtree, *J. Am. Chem. Soc.* **1990**, *112*, 6912.

- <sup>[2]</sup> H. Brunner, in *Applied Homogeneous Catalysis with Organometallic Compounds* (Eds.: B. Cornils, W. A. Herrmann), Verlag Chemie, Weinheim, Germany, **1996**, vol. 1, chapter 2, p. 201.
- <sup>[3]</sup> A. J. Maeland, in *Recent Advances in Hydride Chemistry* (Eds.: M. Peruzzini, R. Poli), Elsevier, Amsterdam, NL, **2001**, chapter 18.
- <sup>[4]</sup> <sup>[4a]</sup> R. Cammack, P. van Vliet, in *Bioinorganic Catalysis* (Eds.: J. Reedijk, E. Bowman), Marcel Dekker, New York, NY, USA, **1998**, chapter 9. <sup>[4b]</sup> R. A. Henderson in *Recent Advances in Hydride Chemistry* (Eds.: M. Peruzzini, R. Poli), Elsevier, Amsterdam, NL, **2001**, chapter 16.
- <sup>[5]</sup> <sup>[5a]</sup> J. B. Arterburn, K. V. Rao, D. M. Goreham, M. V. Valenzuela, M. S. Holguin, K. A. Hall, K. C. Ott, J. C. Bryan, *Organometallics* **2000**, *19*, 1789. <sup>[5b]</sup> E. Deutsch, K. Libson, S. Jurisson, L. F. Lindoy, *Prog. Inorg. Chem.* **1983**, *30*, 75. <sup>[5c]</sup> S. S. Jurisson, J. D. Lydon, *Chem. Rev.* **1999**, *99*, 2205. <sup>[5d]</sup> W. A. Wolkert, T. J. Hoffman, *Chem. Rev.* **1999**, *99*, 2269. <sup>[5e]</sup> J. R. Dilworth, S. J. Parrott, *Chem. Soc. Rev.* **1998**, *27*, 43. <sup>[5f]</sup> F. Tisato, F. Refosco, G. Bandoli, *Coord. Chem. Rev.* **1994**, *135*, 235.
- <sup>[6]</sup> <sup>[6a]</sup> L. Sacconi, F. Mani, *Transition Met. Chem. (NY)* **1982**, *8*, 214. <sup>[6b]</sup> F. Mani, L. Sacconi, *Comments Inorg. Chem.* **1983**, *2*, 157. <sup>[6c]</sup> H. Mayer, W. Kaska, *Chem. Rev.* **1994**, *94*, 1239. <sup>[6d]</sup> F. A. Cotton, B. Hong, *Prog. Inorg. Chem.* **1992**, *40*, 179.
- <sup>[7]</sup> C. Bianchini, M. Peruzzini, F. Zanobini, L. Magon, L. Marvelli, R. Rossi, *J. Organomet. Chem.* **1993**, *451*, 97.
- <sup>[8]</sup> S. C. Abrahams, A. P. Ginsberg, T. F. Koetzle, P. Marsh, C. R. Sprinkle, *Inorg. Chem.* **1986**, *25*, 2500.
- <sup>[9]</sup> M. T. Costello, P. E. Fanwick, M. A. Green, R. A. Walton, *Inorg. Chem.* **1992**, *31*, 2369.
- <sup>[10]</sup> <sup>[10a]</sup> L. Sacconi, I. Bertini, *J. Am. Chem. Soc.* **1967**, *89*, 2235. <sup>[10b]</sup> L. Sacconi, I. Bertini, *J. Am. Chem. Soc.* **1968**, *90*, 5443. <sup>[10c]</sup> L. Sacconi, *Coord. Chem. Rev.* **1972**, *8*, 351. <sup>[10d]</sup> R. Morassi, I. Bertini, L. Sacconi, *Coord. Chem. Rev.* **1973**, *11*, 343.
- <sup>[11]</sup> J. R. Dilworth, D. V. Griffiths, J. M. Hughes, S. Morton, *Inorg. Chim. Acta* **1992**, *196*, 146.
- <sup>[12]</sup> G. Jia, A. J. Lough, R. H. Morris, *J. Organomet. Chem.* **1993**, *461*, 147.
- <sup>[13]</sup> C. Bianchini, A. Meli, M. Peruzzini, F. Vizza, F. Zanobini, *Coord. Chem. Rev.* **1992**, *120*, 193.
- <sup>[14]</sup> C. Mealli, C. A. Ghilardi, A. Orlandini, *Coord. Chem. Rev.* **1992**, *120*, 361.
- <sup>[15]</sup> <sup>[15a]</sup> M. Friebohn, *Basic One- and Two-Dimensional NMR Spectroscopy*, 2nd ed., Verlag Chemie, Weinheim, Germany, **1993**, chapter 11. <sup>[15b]</sup> H. Shanan-Atidi, K. H. Bar-Eli, *J. Phys. Chem.* **1970**, *74*, 961. <sup>[15c]</sup> K. Pihlaja, E. Kleinpeter, *Carbon-13 NMR Chemical Shifts and Stereochemical Analysis*, Verlag Chemie, Weinheim, Germany, **1994**, p. 299–302.
- <sup>[16]</sup> C. Bianchini, M. Peruzzini, A. Polo, A. Vacca, F. Zanobini, *Gazz. Chim. Ital.* **1991**, *121*, 643.
- <sup>[17]</sup> D. Fost, E. H. Carlson, M. Raban, *J. Chem. Soc., Chem. Commun.* **1971**, 656.
- <sup>[18]</sup> V. I. Bakhmutov, E. V. Vorontsov, *Rev. Inorg. Chem.* **1998**, *18*, 183.
- <sup>[19]</sup> R. H. Crabtree, *Acc. Chem. Res.* **1990**, *23*, 95.
- <sup>[20]</sup> P. J. Desrosiers, L. Cai, Z. Lin, R. Richards, J. Halpern, *J. Am. Chem. Soc.* **1991**, *113*, 4173.
- <sup>[21]</sup> D. G. Gusev, A. B. Vymenits, V. I. Bakhmutov, *Inorg. Chem.* **1991**, *30*, 3118.
- <sup>[22]</sup> X.-L. Luo, R. H. Crabtree, *J. Chem. Soc., Dalton Trans.* **1991**, 587.
- <sup>[23]</sup> C. Bianchini, S. Moneti, M. Peruzzini, F. Vizza, *Inorg. Chem.* **1997**, *36*, 5818.
- <sup>[24]</sup> G. G. Hlatky, R. H. Crabtree, *Coord. Chem. Rev.* **1985**, *65*, 1.
- <sup>[25]</sup> C. A. Bayse, M. B. Hall, *J. Am. Chem. Soc.* **1999**, *121*, 3992.
- <sup>[26]</sup> B. A. Patel, J. Wessel, W. Yao, J. C. Lee, T. F. Koetzle, G. P. A. Yap, J. B. Fortin, J. S. Ricci, A. Albinati, O. Eisenstein, A. L. Rheingold, R. H. Crabtree, *New J. Chem.* **1996**, *21*, 413.
- <sup>[27]</sup> R. Bau, M. H. Drabnis, *Inorg. Chim. Acta* **1997**, *259*, 27.
- <sup>[28]</sup> A. Albinati, L. M. Venanzi, *Coord. Chem. Rev.* **2000**, *200*, 687.

- [29] L. M. Epstein, N. V. Belkova, E. S. Shubina, in *Recent Advances in Hydride Chemistry* (Eds.: M. Peruzzini, R. Poli), Elsevier, Amsterdam, NL, **2001**, chapter 14.
- [30] E. S. Shubina, N. V. Belkova, L. M. Epstein, *J. Organomet. Chem.* **1997**, 536–537, 17.
- [31] D. V. Yandulov, K. G. Caulton, N. V. Belkova, E. S. Shubina, L. M. Epstein, D. V. Khoroshum, D. G. Musaev, K. Morokuma, *J. Am. Chem. Soc.* **1998**, 120, 12553 and references therein.
- [32] E. T. Papish, M. P. Magee, J. R. Norton, in *Recent Advances in Hydride Chemistry* (Eds.: M. Peruzzini, R. Poli), Elsevier, Amsterdam, NL, **2001**, chapter 12.
- [33] R. B. Girling, P. Grebenik, *Inorg. Chem.* **1986**, 25, 31.
- [34] D. V. Yandulov, D. Huang, J. C. Huffman, K. G. Caulton, *Inorg. Chem.* **2000**, 39, 1919.
- [35] In order to avoid self-association processes, the concentrations of the various proton-donor reagents were kept in the range 0.01–0.03 M.
- [36] The problem of the metal vs. hydride preference in protonation reactions has been extensively discussed by Norton and co-workers in ref.[32]
- [37] N. V. Belkova, E. S. Shubina, E. I. Gutsul, L. M. Epstein, S. E. Nefedov, I. L. Eremenko, *J. Organomet. Chem.* **2000**, 610, 58.
- [38] E. S. Shubina, N. V. Belkova, E. V. Bakhmutova, E. V. Vorontsov, V. I. Bakhmutov, A. V. Ionidis, C. Bianchini, L. Marvelli, M. Peruzzini, L. M. Epstein, *Inorg. Chim. Acta* **1998**, 280, 302.
- [39] N. V. Belkova, E. V. Bakhmutova, E. S. Shubina, C. Bianchini, M. Peruzzini, V. I. Bakhmutov, L. M. Epstein, *Eur. J. Inorg. Chem.* **2000**, 2163.
- [40] V. I. Bakhmutov, E. V. Bakhmutova, N. V. Belkova, L. M. Epstein, E. S. Shubina, E. V. Vorontsov, C. Bianchini, D. Masi, M. Peruzzini, F. Zanobini, *Can. J. Chem.* **2001**, 79, 479.
- [41] E. Scharrer, S. Chang, M. Brookhart, *Organometallics* **1995**, 14, 5686.
- [42] E. S. Shubina, A. N. Krylov, N. V. Belkova, L. M. Epstein, A. P. Borisov, V. D. Mahaev, *J. Organomet. Chem.* **1995**, 439, 275.
- [43] E. S. Shubina, L. M. Epstein, *Ber. Bunsenges. Phys. Chem.* **1998**, 102, 359.
- [44] K. Abdur-Rashid, T. P. Fong, B. Greaves, D. G. Gusev, J. G. Hinman, S. E. Landau, A. J. Lough, R. H. Morris, *J. Am. Chem. Soc.* **2000**, 122, 9155.
- [45] The empirical rule of factors reported by Iogansen<sup>[46]</sup> demonstrates the invariability of the proton-donor ( $P_i$ ) and proton-acceptor ( $E_j$ ) properties of organic acids and bases in hydrogen bonding. In Equation (5),  $\Delta H_{11}$  is the enthalpy of hydrogen bonding for a standard donor/acceptor couple (i.e. PhOH/Et<sub>2</sub>O:  $P_i = E_i = 1$ ).  $E_j$  depends on neither the nature of the proton donor nor the solvent and may therefore be assumed as an absolute measurement of the proton-accepting ability of each potential site of hydrogen bonding.<sup>[30]</sup>
- [46] A. V. Iogansen, *Theor. Experim. Khim.* **1971**, 7, 302.
- [47] G. Orlova, S. Scheiner, *J. Phys. Chem. A* **1998**, 102, 4813.
- [48] R. Morassi, L. Sacconi, *Inorg. Synth.* **1976**, 16, 174.
- [49] J. Chatt, R. J. Dosser, F. King, G. J. Leigh, *J. Chem. Soc., Dalton. Trans.* **1976**, 2436.
- [50] A. C. T. North, D. C. Philips, F. S. Mathews, *Acta Crystallogr., Sect. A* **1968**, 24, 351.
- [51] *MOLEN: Molecular Structure Solution Procedure*, Enraf–Nonius, Delft, The Netherlands, **1990**.
- [52] *International Tables for X-ray Crystallography*, Kynoch Press, Birmingham, England, **1974**, vol. IV.
- [53] C. K. Johnson, *ORTEP II*, Report ORNL-6138, Oak Ridge National Laboratory, Oak Ridge, TN, **1976**.

Received November 2, 2001

[101470]